

This is an electronic reprint of the original article. This reprint may differ from the original in pagination and typographic detail.

Clays catalyzed cascade Prins and Prins-Friedel-Crafts reactions for synthesis of terpenoid-derived polycyclic compounds

Sidorenko, A. Yu; Kurban, Yu M.; Kravtsova, A. V.; Il'ina, I. V.; Li-Zhulanov, N. S.; Korchagina, D. V.; Sánchez-Velandia, J. E.; Aho, A.; Volcho, K. P.; Salakhutdinov, N. F.; Murzin, D. Yu; Agabekov, V. E.

Published in:
Applied Catalysis A: General

DOI:
[10.1016/j.apcata.2021.118395](https://doi.org/10.1016/j.apcata.2021.118395)

Published: 05/01/2022

Document Version
Accepted author manuscript

Document License
CC BY-NC-ND

[Link to publication](#)

Please cite the original version:

Sidorenko, A. Y., Kurban, Y. M., Kravtsova, A. V., Il'ina, I. V., Li-Zhulanov, N. S., Korchagina, D. V., Sánchez-Velandia, J. E., Aho, A., Volcho, K. P., Salakhutdinov, N. F., Murzin, D. Y., & Agabekov, V. E. (2022). Clays catalyzed cascade Prins and Prins-Friedel-Crafts reactions for synthesis of terpenoid-derived polycyclic compounds. *Applied Catalysis A: General*, 629, Article 118395. <https://doi.org/10.1016/j.apcata.2021.118395>

General rights

Copyright and moral rights for the publications made accessible in the public portal are retained by the authors and/or other copyright owners and it is a condition of accessing publications that users recognise and abide by the legal requirements associated with these rights.

Take down policy

If you believe that this document breaches copyright please contact us providing details, and we will remove access to the work immediately and investigate your claim.

Clays catalyzed cascade Prins and Prins-Friedel-Crafts reactions for synthesis of terpenoid-derived polycyclic compounds

A.Yu. Sidorenko^{a*}, Yu.M. Kurban^a, A.V. Kravtsova^a, I.V. Il'ina^b, N.S. Li-Zhulanov^b, D.V. Korchagina^b, J.E. Sánchez-Velandia^c, A. Aho^d, K.P. Volcho^b, N.F. Salakhutdinov^b, D.Yu. Murzin^{d*}, V.E. Agabekov^a

^aInstitute of Chemistry of New Materials of National Academy of Sciences of Belarus, 220141, Skaryna str, 36, Minsk, Belarus

^bNovosibirsk Institute of Organic Chemistry, Lavrentjev av. 9, 630090, Novosibirsk, Russian Federation

^cCentro de Investigaciones en Catálisis, Universidad Industrial de Santander, Escuela de Química, km.2. vía El Refugio, 680006, Piedecuesta, Santander, Colombia.

^dÅbo Akademi University, Biskopsgatan 8, 20500 Turku/Åbo, Finland

Corresponding authors

Dr. A.Yu. Sidorenko

e-mail: Sidorenko@ichnm.by;

Tel: +375 17 268 63 08

Address: Institute of Chemistry of New Materials of National Academy of Sciences of Belarus, 220141, Skaryna str, 36, Minsk, Belarus

Professor Dr. D.Yu. Murzin

Åbo Akademi University

Biskopsgatan 8, 20500, Turku/Åbo, Finland

Tel: + 358 2 215 4985

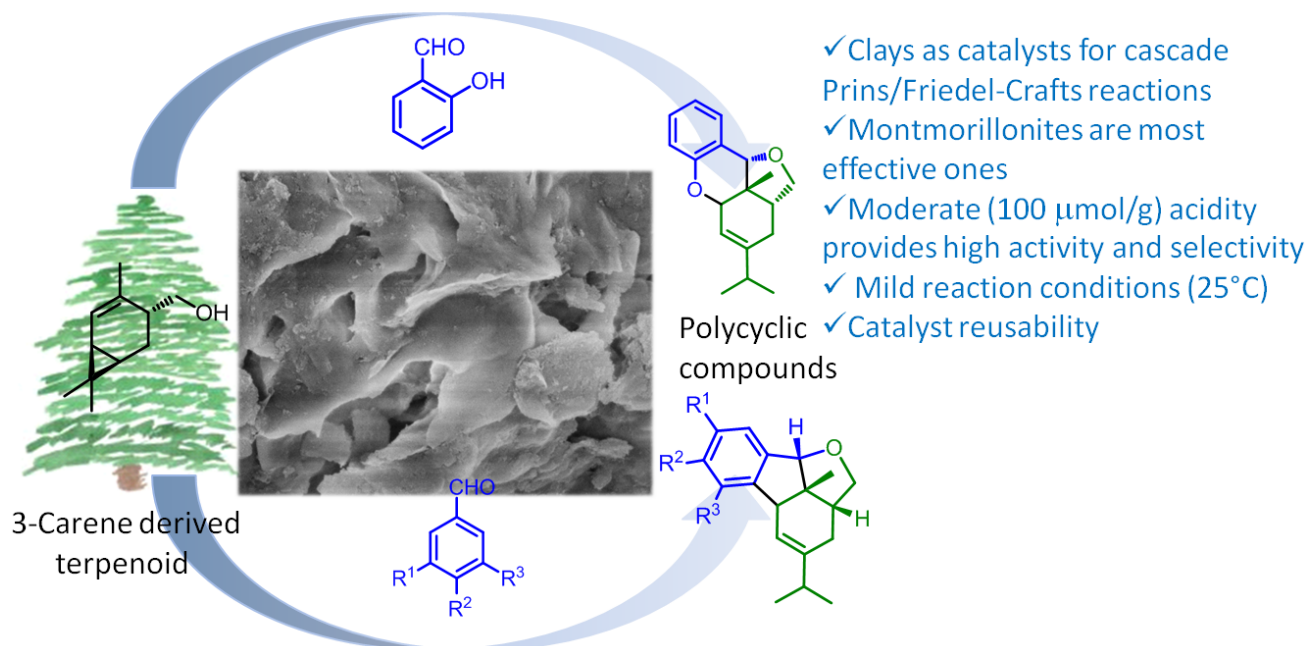
e-mail: dmitry.murzin@abo.fi

Abstract

The Prins/Friedel-Crafts cascade reactions of the terpenoid *trans*-4-hydroxymethyl-2-carene (synthesized from 3-carene) with aromatic aldehydes were systematically studied for the first time on acidic mesoporous clays (halloysite, illite, montmorillonites). Both the reaction rate and selectivity to the desired polycyclic product with tetrahydrofuran moiety increased with an increase in the catalyst acidity and their drying temperature, indicating that relatively strong Brønsted and Lewis acid sites favored their formation. The best activity and selectivity (up to 97%) was demonstrated over commercial montmorillonite K-10 with acidity of *ca.* 100 $\mu\text{mol/g}$. In contrast, on strongest acids (resin Amberlyst-15), dehydration/aromatization of the substrate was observed. It was shown, that mesoporosity of the catalyst is one of the key factors governing catalytic behavior. The presence of at least one an electron-donor substituent at the *meta*-position of benzaldehyde is critical for the Prins-Friedel-Crafts reaction. Overall, available montmorillonites are an effective replacement for homogeneous catalysts for the Prins/Friedel-Crafts cascade reactions.

Keywords: Cascade reactions; Prins/Friedel-Crafts; Clays; Terpenoids, Polycyclic compounds

Graphical abstract



1. Introduction

It is known that compounds with a tetrahydrofuran moiety have a variety of biological activities [1–3]. For example, polycyclic tetrahydrofurans and their derivatives have high cytotoxic [3–5], anti-inflammatory [3, 6] and fungicidal effects [7], and can also be used as fragrant substances [6].

Cascade (tandem) reactions are an effective method for the synthesis of polycyclic compounds, the main advantage being sequential formation of several chemical bonds in one reaction space, which eliminates a need for isolation and purification of intermediate products [8–11].

Although the Prins reaction *per se* is well known, the Prins-initiated cascade transformations are much less studied [8, 9]. For example, unsaturated alcohols *trans*-4-phenyl-but-3-en-1-ol and *trans*-4-hydroxymethyl-2-carene can undergo the tandem Prins condensation with salicylic aldehyde to form furanochromene compounds (Fig. 1a) in yields up to 88% [7, 12, 13]. The reaction of benzaldehyde with the above alcohols leads to formation of multicomponent mixtures of products [13, 14], while the presence of electron-donor substituents at the 3, 4, and 5 positions of the benzene ring makes it possible for a cascade Prins-Friedel-Crafts reaction (Fig. 1b) with the formation of polycyclic compounds with the tetrahydrofuran moiety [13–15]. Their yields were up to 92% [13–15], sharply decreasing to 16% in the absence of a substituent in the *m*-position of the aromatic aldehyde ($R^1 = H$) [13].

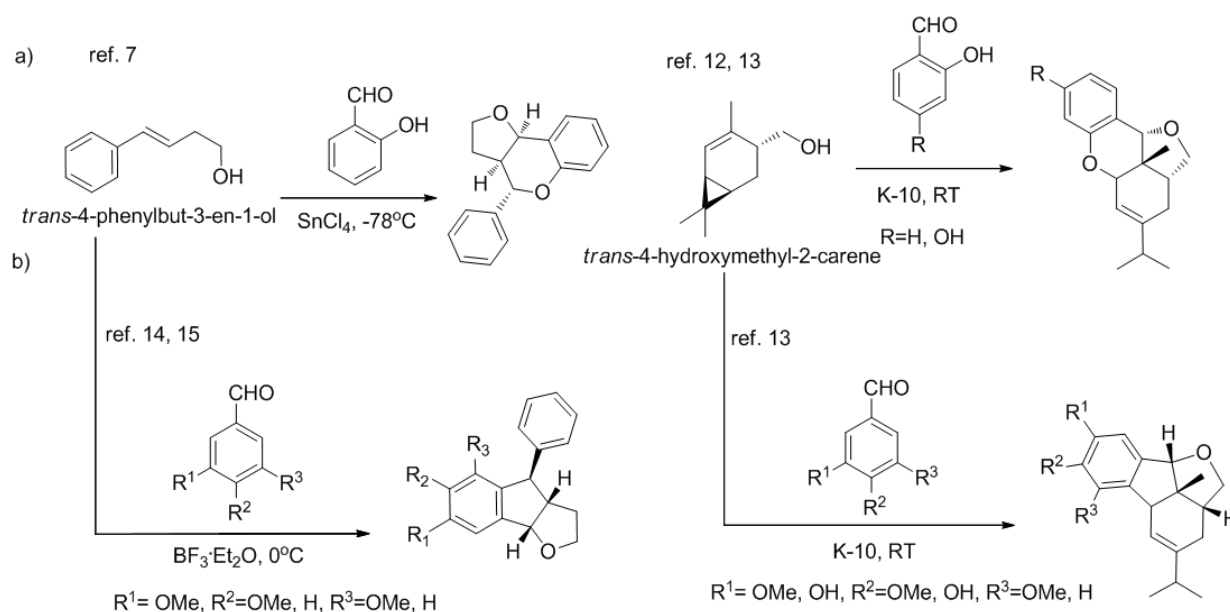


Fig. 1. Examples of Prins (a) and Prins-Friedel-Crafts (b) cascade reactions for the synthesis of polycyclic compounds with a tetrahydrofuran moiety

their physicochemical and textural properties as well as the influence of the activation conditions on the reaction pathways.

However, the concentration and strength of acid sites play a significant role in the Prins-type reactions. For example, the selective isopulegol condensation with thiophene-2-carbaldehyde to the octahydro-2*H*-chromene-4-ols requires weak Brønsted a.s. [32]. On the contrary, the tandem reaction of this terpenoid with benzaldehyde and acetonitrile proceeds over much stronger SO₃H-groups [29]. The formation of 2,5-dimethyl-hexadiene by isobutanal-isobutene Prins condensation occurs selectively on relatively weak acids [33]. The three-component reaction butyraldehyde, 3-butene-1-ol and anisole to 4-aryltetrahydropyrans requires medium-strength Brønsted a.s. [31]. Therefore, it is necessary to develop effective catalysts for each specific reaction.

At the same time, no systematic studies of cascade transformations in the presence of materials with different structures, nature and strength of acid sites, as well as the conditions for activating catalysts and carrying out the 4-hydroxymethyl-2-carene cascade reactions with aldehydes have been performed.

Clays, which mainly consist of layered aluminosilicates, are readily available and environmentally friendly heterogeneous catalysts for a number of organic reactions [34, 35]. One of the effective methods for activating clays is acid treatment, which leads to an increase in their acidity because of cation exchange, as well as porosity and specific surface area due to leaching of the metal cations from the structure of these minerals [36]. Most often, montmorillonite clays are subjected to acid modification, because the resulting products have a relatively high specific surface area and porosity [36]. For example, there is a commercially available acid-activated montmorillonite K-10, which can be used in organic synthesis [35]. A promising material for creating novel catalytic systems is also the clay mineral halloysite, which morphologically represents multilayer aluminosilicate nanotubes [37]. Thus, it has recently been shown that halloysite nanotubes (HNT) modified with HCl are highly selective catalysts for the Prins reaction used to synthesize compounds with chromene and isobenzofuran structures based on terpene compounds (-)-isopulegol and 2-carene [32, 38].

This work is devoted to the study of the catalytic properties of a number of acid-treated clays (montmorillonite, illite, halloysite) in the Prins and Prins-Friedel-Crafts cascade reactions using as an example of the of *trans*-4-hydroxymethyl-2-carene **1** condensation with salicylic aldehyde, as well as 3,4,5-trimethoxybenzaldehyde under various conditions for the synthesis of polycyclic compounds with the tetrahydrofuran moiety. The reaction scope and catalyst reusability have also been studied.

2. Experimental

All commercial materials and reagents used were purchased from Sigma-Aldrich. 4-Hydroxymethyl-2-carene **1** was synthesized from (+)-3-carene according to a published procedure [18] with some modification and had a purity of 87% (including 5% of the *cis*-isomer). A detailed procedure for the synthesis of compound **1** is presented in Supplementary Information (SI).

2.1. Preparation and characterization of catalysts

The materials studied in this work were halloysite (Dragon Mine, USA), illite (Russia), and commercial acid-modified montmorillonites K-10 and K-30 (Germany). For comparison, the strong Lewis ($\text{BF}_3 \cdot \text{Et}_2\text{O}$) and Brønsted (Amberlyst-15) acids, as well as zeolite H-Beta-300 were used.

Clays K-10 and K-30 were used without any additional chemical treatment. Acid modification of halloysite and illite was carried out according to the following procedure [36]. A portion of the clay (*ca.* 7 g) was introduced into a three-necked flask, to which a 10% solution of HCl (5.0 mL of acid per 1.0 g of the solid phase) was then added, heated to 90°C, and treated under these conditions for 3.0 h with continuous stirring (300 rpm). Then the precipitate was thoroughly washed with distilled water until there were no Cl^- ions in the washings, dried at 105°C to a constant weight, and ground to a particle size of <100 μm .

The specific surface area (S_{BET}) and porosity of the solids were investigated on ASAP 2020 MP (Micromeritics) equipment for which the samples were evacuated for 1 h at 200°C (residual pressure 0.013 Pa). The volume (V_{pore}) and the average diameter (D_{pore}) of the pores were determined by the standard BJH method using the desorption branch of the isotherm [39]. Energy dispersive X-ray spectroscopy (electron microscope JEOL JCM-6000Plus with chemical analysis system) was applied to determine the chemical composition of clays.

The type and concentration of acid sites (a.s.) of the clays were determined by FTIR spectroscopy with pyridine as a probe molecule [40]. The samples were pretreated at 350°C (1 h), then cooled to 100°C and saturated with pyridine at this temperature for 30 min. To determine the concentration of weak, medium, and strong a.s., FTIR spectra were recorded at 150°C, medium and strong a.s. at 250°C, while strong ones at 350°C [41]. The Lewis and Brønsted acidity were identified by the characteristic absorption bands at 1450 cm^{-1} and 1545 cm^{-1} , respectively; their amounts were calculated using the Emeis molar extinction coefficients [42].

The morphology of the clays was studied by scanning electron microscopy (SEM) on a Zeiss Leo 1530 microscope. It is necessary to note that hydrochloric acid-modified halloysite nanotubes (HNT) were characterized by a wide range of methods including MAS NMR, SEM, TEM, FTIR with pyridine in the early study of the authors [32].

2.2. Reaction and analysis of products

Typically, the reaction of *trans*-4-hydroxymethyl-2-carene **1** with aldehydes was carried out as follows. Substrate **1** (0.35 g, 1.85 mmol), an equivalent amount of aldehyde, and a solvent

(methylene chloride) were introduced into a three-necked flask with magnetic stirrer. The total volume of the mixture was 5.0 mL, unless otherwise indicated. After setting the required temperature (25°C), the catalyst (1.0 g) was added and stirring (400 rpm) was started.

To determine the composition of the reaction mixture, the samples were periodically taken; ethyl acetate was added to them to extract products from the catalyst surface, and analyzed using a gas chromatograph Khromos GKh-1000 with a flame ionization detector and a Zebron ZB-5 capillary column (30 m x 0.25 mm x 0.25 μm). The evaporator and detector temperature were 250 and 280°C respectively. The column heating was implemented according to the following program: holding for 1 min at 110°C, temperature rise from 110 to 280°C at with the ramp of 20°C/min, then isothermal mode for 25 min. An internal standard (dodecanol, 99.0%) and product samples were used for quantitation. Typical chromatograms of the reaction products are shown in Fig. S2.

Separation of the reaction mixtures was carried out by preparative column chromatography. The structures of the obtained compounds were established by ¹H and ¹³C NMR spectroscopy and high-resolution mass spectrometry. Detailed techniques for isolating and analyzing product structure are given in the Supplementary Information.

2.3. DFT study

The optimizations of the structures were performed at the DFT level using the hybrid functional of the electronic density Perdew-Burke-Ernzerhoff, PBE (considering computational costs, accuracy and coverage of the results, as it was previously reported) with the 6-311++G(d,p) basis set [43]. All computational runs were carried out with the Gaussian09 program [44, 45]. It is well known that standard DFT methods fail to describe the non-local nature of the substances towards the van der Waals interactions [46]. For this, the empirical dispersion correction of Grimme (D3) was considered during the frequencies calculations [47]. After optimization of the structures, additional runs were performed at m062x level (Minnesota functionals) with a change of the basis set (6-31g(d,p)) for improving values of energies and for obtaining thermodynamic values of each reaction [48]. Minimal structures were verified with the frequencies values obtained after optimization. Furthermore, such frequencies were also calculated and verified using analytic second derivatives of the energy, which confirm the nature of the stationary point. The solvation effects (CH₂Cl₂) were included and computed at the same level of theory on the optimized structure towards the conductor-like polarizable continuum model (CPCM) implemented in the Gaussian09 package. The model involves the solute cavity via a set of overlapping spheres, using a continuous surface charge formalism that ensures continuity and robustness of the reaction [49]. As the proton source H₃O⁺ was chosen because these species largely determine the Brønsted acidity of clays [50].

3. Results and Discussion

3.1. Physicochemical characteristics of clays

The acid-treated halloysite contains mainly alumina (32.1%) and silica (66.9%). In modified illite, the Al₂O₃ content is significantly lower (19.8%); the presence of significant amounts of iron and potassium oxides was also observed. The chemical composition of commercial montmorillonites K-10 and K-30 is practically the same, namely these clays contained the smallest amount of Al₂O₃ (14.4 –15.7%) while the SiO₂ content reaches 80.5% (Table 1).

The specific surface area values for halloysite and illite after treatment with 10% HCl increased significantly (up to 167 m²/g), but were lower than those for commercial acid-modified montmorillonites K-10 and K-30 (up to 247 m²/g). The nitrogen adsorption-desorption isotherms for the studied clays had a hysteresis loops characteristic for the mesoporous materials (Fig. S1, Supplementary Information), while the mean pore diameters of the solids ranged from 5.1 to 10.1 nm (Table 1).

Table 1. Chemical composition and porous structure of the investigated clays

Clay	Chemical composition, wt. %								Porous structure		
	Al ₂ O ₃	SiO ₂	FeO	Na ₂ O	MgO	K ₂ O	CaO	TiO ₂	S _{BET} , m ² /g	V _{vore} , cm ³ /g	D _{pore} , nm
Halloysite											
initial	44.1	54.4	0.5	0.2	0.1	-	0.4	0.3	60	0.22	15.7
acid-modified*	32.1	66.9	0.3	0.1	0.1	-	0.1	0.4	167	0.40	10.1
Illite											
initial**	19.5	54.7	10.6	0.7	2.9	4.7	5.8	1.2	46	0.10	8.1
acid-modified*	19.8	64.4	6.4	0.1	1.7	5.6	0.1	1.9	146	0.28	8.1
K-10	15.7	77.9	2.8	0.2	1.9	0.9	0.4	0.2	247	0.36	5.1
K-30	14.4	80.5	2.1	0.1	1.5	0.8	0.3	0.3	240	0.40	6.9

*The data from *[32] and **[41]

The images of scanning electron microscopy of halloysite (Fig. 3a) show typical nanosized tubes which are characteristic for this kind of minerals [32, 37]. Illite is represented by irregularly shaped lamellar particles (Fig. 3b), while montmorillonites are morphologically characterized by cloud-like aggregates (Fig. 3c,d).

Illite and montmorillonite are representatives of the 2:1 clay minerals (Fig. S3a), the layer of which consists of two silica-oxygen tetrahedral sheets with one alumina-oxygen octahedral sheets between them [36, 50]. These minerals are characterized by partial isomorphous substitution of Al³⁺

for Si^{4+} in tetrahedra and Mg^{2+} , $\text{Fe}^{2+/3+}$ for Al^{3+} in octahedra [50]. The resulting negative charge is compensated by the interlayer cations. Halloysite belongs to the 1:1 structural type, the layer of which is a combination of tetrahedral Si – O and octahedral Al – O sheets (Fig. S3b), isomorphism in which is practically absent [32, 37].

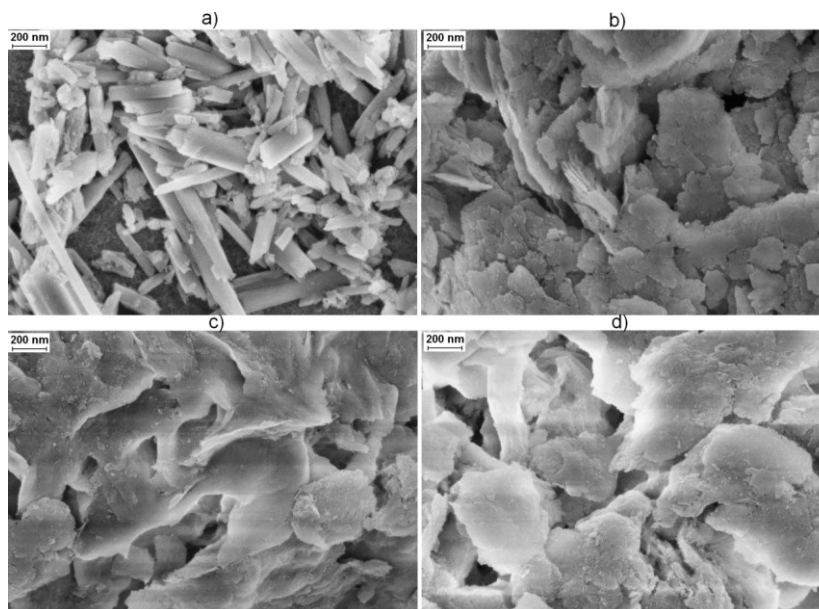


Fig. 3. SEM images of modified clays: halloysite (a), illite (b), montmorillonites K-10 (c) and K-30 (d)

Detailed description of the differences in the structure of acid-modified halloysite, illite, and montmorillonite by ^{29}Si and ^{27}Al NMR spectroscopy were presented previously [32, 41]. Thus, the ^{29}Si NMR spectra of the studied clays exhibit characteristic peaks at about -92 ppm, which refer to the initial fragments of their structure $\text{Si}(\text{OSi})_3$, where one silicon-oxygen tetrahedron is linked to three analogous ones [32, 41, 51]. The signals with maxima in the range from -86 to -90 ppm in the illite and montmorillonite K-10 spectra (Fig. 4b,c) characterize the isomorphic substitution of one Al^{3+} for Si^{4+} in their tetrahedral sheets [41, 51], i.e. correspond to $\text{Si}(\text{OSi})_2(\text{OAl})$ units.

Peaks at about -101 ppm are associated with the presence of $\text{Si}(\text{OSi})_3(\text{OH})$ fragments in clays, which are formed during their acid modification by Si–O–Al bonds breaking between tetrahedral and octahedral sheets [32, 41, 51]. The signals of *ca.* -111 ppm indicate the presence of $\text{Si}(\text{OSi})_4$ units, i.e. amorphous SiO_2 formed upon crosslinking of $\text{Si}(\text{OSi})_3(\text{OH})$ fragments in an acidic medium [32, 41, 51]. Maxima at -107 ppm in the ^{29}Si MAS NMR spectra of illite and montmorillonite K-10 indicate the presence of quartz as an impurity [41, 51].

The ^{27}Al NMR spectra of the studied clays (Fig. 4) show characteristic intense peaks with maxima in the range from 4.0 to 5.2 ppm, which reflect the presence of six-coordinated aluminum

(Al^{VI}) in their octahedral layers [32, 41, 51]. The spectra of illite and montmorillonite also show weak signals in the range from 50 to 80 ppm, which are related to four-coordinated aluminum (Al^{IV}) present in the tetrahedral layers of these clays because of isomorphous substitution of n Al³⁺ for Si⁴⁺ [41, 51].

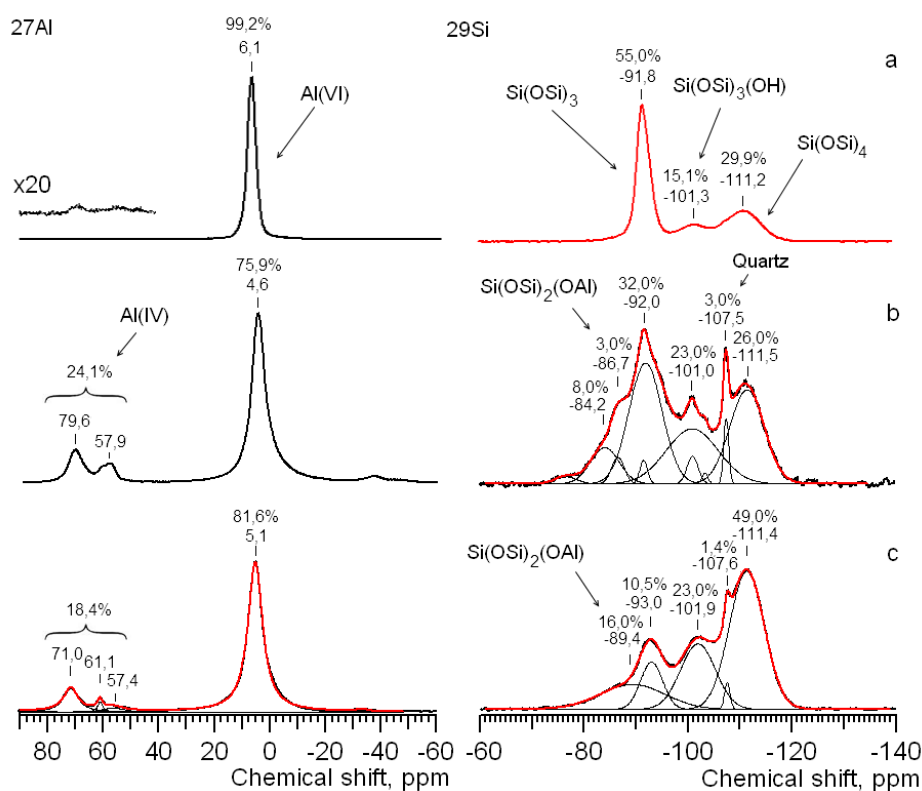


Fig. 4. ²⁹Si and ²⁷Al MAS NMR spectra treated with 10% HCl (a) halloysite, and (b) illite, and (c) commercial montmorillonite K-10 (modified from [32, 41])

The destruction of illite after treatment with 10% HCl was more pronounced than for halloysite nanotubes, as indicated by a higher (55%) content of the initial Si(OSi)₃ units in the latter (Fig. 4a,b). Commercial montmorillonite K-10 was characterized by an even lower content of the pristine fragments; it was dominated (72%) by the Si(OSi)₃(OH) and Si(OSi)₄ units, which were formed as a result of acidic destruction of the clay. It is known that the acid action on montmorillonite leads to disordering of its laminar structure, with the formation of interlayers of amorphous SiO₂ [36, 50]; therefore, its specific surface after treatment is higher than that for illite and halloysite (Table 1).

According to FTIR with pyridine, the concentration of acid sites (a.s.) in acid-modified samples of HNT and illite (up to 63 μmol/g) was significantly lower than that for commercial montmorillonites K-10 and K-30 (up to 104 μmol/g, Table 2). Halloysite and illite were characterized by a predominance of weak (W) a.s. while montmorillonites contained a significant

amount of medium (M) and strong (S) acid sites. Also note that Lewis acidity prevailed in halloysite and montmorillonites (Table 2).

Table 2. Acidic properties of the investigated solids

Acid-modified clay	Concentration of acid sites, $\mu\text{mol/g}$						L/B	W/(M+S)	
	Brønsted (B)			Lewis (L)					
	Weak (W)	Medium (M)	Strong (S)	Weak (W)	Medium (M)	Strong (S)			
Halloysite*	13.0	6.0	0	21.0	12.0	0	52.0	1.8	1.9
Illite	15.0	19.0	3.0	19.0	7.0	0	63.0	0.7	1.2
K-10**	15.0	26.0	7.0	35.0	14.0	7.0	104.0	1.2	0.9
K-30**	17.0	17.0	8.0	28.0	24.0	6.0	100.0	1.4	0.8

The data from *[32] and **[41]

Structural features and the isomorphism phenomenon in the studied clays are the reason for differences in their acidity. Thus, according to ^{27}Al MAS NMR data (Fig. 4b,c), 24.1% of Al^{3+} atoms in illite and 18.4% of these species in K-10 are located in tetrahedral (Si–O) sheets. For this reason, a negative charge appears on the layers surface, which is compensated by cations, including H_3O^+ [50]. In illites, exchangeable cations are found mainly on the surfaces of particles, while in montmorillonites also in the interlayer space [50], which is the reason for a higher acidity of K-10 and K-30 clays (Table 2). In halloysite, aluminum atoms are almost completely in the six coordinated state (Fig. 4a), i.e. in octahedral sheets, which means a balance of charges between octa- and tetrahedral sheets. Therefore, acid sites in this mineral should be localized mainly at the ends and defects of nanotubes, and their concentration and strength are lower than in montmorillonites (Table 2).

3.2. Cascade Prins reaction

3.2.1 Influence of the catalyst type

Condensation of *trans*-4-hydroxymethyl-2-carene **1** with salicylic aldehyde **2** led to the formation of a compound with xanthene **3**, as well as isobenzofuran **4** and **5** structures, however, the main product over the studied clays was polycyclic compound **3** (Table 3).

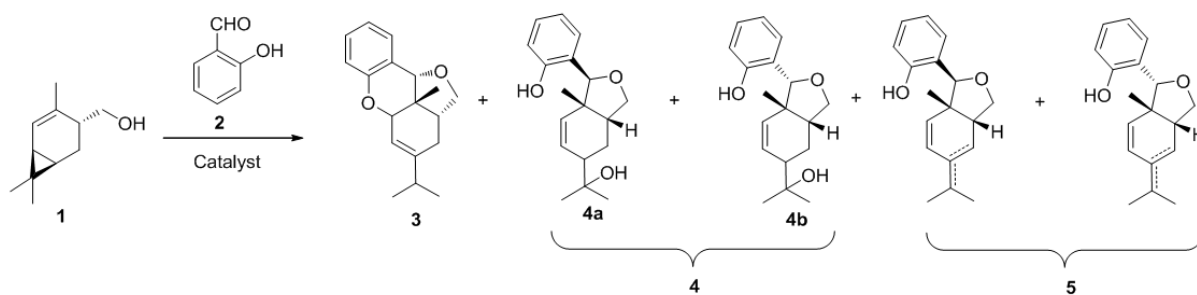


Fig. 5. Reaction of *trans*-4-hydroxymethyl-2-carene with salicylic aldehyde

At 50% of terpenoid **1** conversion the selectivity to compound **3** on montmorillonites K-10 and K-30 (up to 67.1%) was slightly higher than on halloysite and illite catalysts (up to 64.9%, Table 3). At the same time, a larger yield of isobenzofurans **4** (11.4%) was observed on halloysite. In all cases, the conversion of **1** (X_1) was higher than that for aldehyde **2** (conversion X_2), indicating that compound **1** also undergoes side reactions.

Table 3. Acidity and catalytic properties of studied catalysts in *trans*-4-hydroxymethyl-2-carene reaction* with salicylic aldehyde at 25°C

Catalyst	Acidity, $\mu\text{mol/g}$	r_0 , $\text{mmol/g}\cdot\text{min}$	TOF, min^{-1}	Time, min	Selectivity, mol. %			X_2/X_1
					3	4	5	
Halloysite	52.0	0.15	2.8	120	64.9	11.4	3.9	0.75
Illite	63.0	0.05	0.8	180	58.9	11.0	4.6	0.73
K-10	104.0	0.40	3.8	10	65.8	7.5	3.3	0.79
K-30	100.0	0.52	5.2	7	67.1	7.2	3.4	0.78
$\text{BF}_3\cdot\text{Et}_2\text{O}^{**}$	-	-	-	180	47.4	9.4	7.7	0.78
Amberlyst-15	-	0.1	-	30	7.2	1.1	12.3	0.38
H-Beta-300	112.0	No condensation						

Reaction conditions: 1.85 mmol of each reagent, 1.0 g of the catalyst dried 2.0 h at 105°C, temperature 25°C, initial concentration of reagents was 0.37 mol/l. *At 50% conversion; **1.0 eq, at 0°C and 23% conversion for 3.0 h.

The initial consumption rates of terpenoid **1** (r_0) on K-10 and K-30 were significantly higher than those for illite and halloysite, which may be related to a higher concentration of a.s. in montmorillonites (Table 3). The TOF values for the latter catalysts were also the highest.

In the presence of Lewis acid $\text{BF}_3\cdot\text{Et}_2\text{O}$, traditionally used for the Prins reaction [8, 9], the selectivity towards xanthene **3** was significantly lower (47.4%) than on clays (up to 67.1%, Table 3). When using a strong Brønsted acid (resin Amberlyst-15), a multicomponent mixture of products was formed, and the yield of compound **3** was insignificant (7.2%). On zeolite H-Beta-300 (acidity 112

$\mu\text{mol/g}$ [52]), the condensation of compound **1** with salicylic aldehyde did not occur, which may be due to its small pore size (0.76 nm [40]), which is much smaller than in the studied clays (6.9–15.7 nm, Table 1). On the other hand, the Prins-Friedel-Crafts cascade reaction between butyraldehyde, 3-buten-1-ol and anisole proceeded efficiently in the presence of hierarchical Beta zeolites (silica to alumina ratio of 25), which was due to the presence in them a developed system of mesopores and moderately strong Brønsted a.s. [31].

Note that almost complete conversion of terpenoid **1** (up to 96%) for 5.0 h of reaction was observed on montmorillonites, whereas in the presence of modified halloysite and illite, it did not exceed 58% (Table S1).

Thus, mesoporous clays with medium acidity (*ca.* 100 $\mu\text{mol/g}$), namely commercial montmorillonites K-10 and K-30, are effective catalysts for the Prins cascade reaction of *trans*-4-hydroxymethyl-2-carene with salicylic aldehyde.

3.2.1 Influence of reaction conditions

An increase in the drying temperature of montmorillonite led to an increase in the initial rate of consumption of terpenoid **1**, its conversion for 5 h of the reaction, as well as in selectivity to xanthene **3** (Table 4). Thus, the highest yield of **3** (79.7%) was observed after thermal treatment of clay at 350°C, while the initial reaction rate was maximum in the case of its drying at 150°C. Also note an increase in the X_2/X_1 conversion ratio with an increase in the catalyst thermal activation, which indicates that the reagent **1** undergoes secondary transformations on K-10 clay treated at low temperatures.

Similarly, an increase in the drying temperature of halloysite nanotubes led to an increase in the initial consumption rate of **1** and selectivity to polycyclic product **3** reaching 69.4% after treatment at 200°C (Table S2). However, under the same drying conditions, the yield of product **3** over HNT was lower than for K-10 (Table 4 and S2).

Table 4. Selectivity in 4-*trans*-hydroxymethyl-2-carene reaction with salicylic aldehyde on K-10 after 5 h

K-10 drying temperature, °C	r_0 , mmol/g·min	Conversion of 1 , mol. %	Selectivity, mol. %			X_2/X_1
			3	4	5	
50	0.015	38.7	53.0	16.1	4.7	0.70
105	0.40	93.8	66.5	7.6	6.5	0.79
150	0.50	93.9	71.1	7.8	6.2	0.82
200	0.25	89.9	72.9	8.6	5.2	0.83
350	0.30	91.3	79.7	8.4	6.1	0.86

Reaction conditions: 1.85 mmol of each reagent, 1.0 g of the catalyst, temperature 25°C, initial concentration

of reagents was 0.37 mol/l

An increase in selectivity to xanthene **3** as a result of an increase in the catalysts drying temperature can be explained by a change in the nature and strength of their acid sites during such thermal treatment. Thus, the acidity of clays is determined by exchangeable and coordination-unsaturated cations (Lewis a.s.), acidic hydroxyl groups, and water molecules bound with exchange cations (for example Al^{3+}) on the surface and in the interlayer space (Brønsted a.s.) [50, 53].

The studied halloysite and montmorillonites are characterized by both types of acidity with a prevalence of Lewis a.s. (Table 2). As a result of clays heat treatment, a partial dehydration of their surface occurs, leading to an increase in the concentration and strength of a.s. [50, 53]. According to [54], the largest Brønsted acidity of clays was observed after drying at 150°C, while Lewis acidity dominant as a result of thermal activation at 250–300°C. Consequently, the formation of the Prins cascade reaction product, xanthenes **3**, is favored by a relatively strong Brønsted or Lewis acidity of clays.

With an increase in the reaction temperature from 15 to 35°C the selectivity towards xanthene **3** on montmorillonite K-10 at 50% conversion of the reagent **1** decreased from *ca.* 72 to 61%, respectively (Table 5). At the same time, selectivity to isobenzofurans **4** and **5** was practically independent of the reaction temperature. Based on this, it can be concluded that the product **3** undergoes secondary transformations, probably resinification. Indeed, selectivity to **3** slightly decreased with an increase in conversion of terpenoid **1** and dropped sharply after more than 90% of **1** underwent a reaction at 35°C (Fig. 6).

The apparent activation energy, calculated from the initial consumption rates of compound **1** (Table 7) in Arrhenius coordinates (Fig. S4), was 30.4 kJ/mol, which was lower than that (55.0 kJ/mol) in the case of (-)-isopulegol Prins cyclization with thiophene-2-carbaldehyde to chromene alcohols [32].

Table 5. Selectivity in 4-*trans*-hydroxymethyl-2-carene* reaction with salicylic aldehyde on K-10 depending on reaction temperature

Reaction temperature, °C	r_0 , mmol/(g·min)	Time, min	Selectivity, mol. %			X_2/X_1
			3	4	5	
15	0.25	30	71.7	7.8	3.9	0.80
25	0.40	10	65.8	7.5	3.4	0.79
35	0.57	5	60.8	8.6	4.5	0.82

Reaction conditions: 1.85 mmol of each reagent, 1.0 g of the catalyst dried 2.0 h at 105°C, initial concentration of reagents was 0.37 mol/l. *At 50% conversion

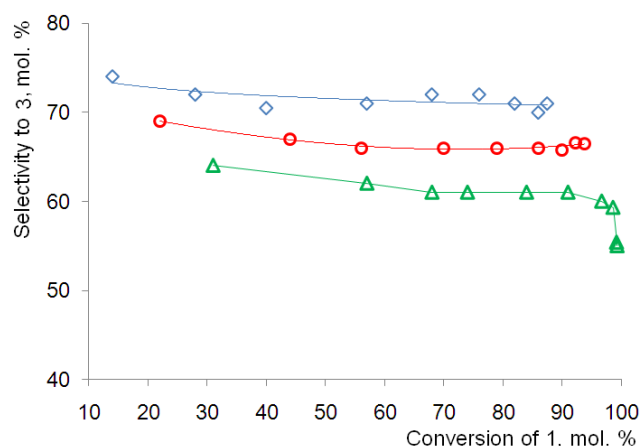


Fig. 6. Selectivity to product **3** as a function of terpenoid **1** conversion at 15°C (\diamond); 25°C (\circ), and 35°C (Δ)

A decrease in the initial concentration of *trans*-4-hydroxymethyl-2-carene **1** from 0.74 to 0.06 mol/L led to a decrease in the selectivity towards product **3** from 66.2 to 54.2%, respectively (Table 6). In all cases, almost complete conversion of **1** was observed after 5 h of the reaction (Table 8), the kinetic curves are shown in Fig. S6.

Table 6. Selectivity in *trans*-4-hydroxymethyl-2-carene reaction with salicylic aldehyde after 5 h of de reaction on K-10* with different initial concentration of reagents

Initial concentration of 1 , mol/L	Conversion of 1 , mol. %	Selectivity, mol. %			X_2/X_1
		3	4	5	
0.74	97.5	66.2	9.4	6.4	0.81
0.37	93.8	66.5	7.6	6.5	0.79
0.18	97.1	64.1	5.0	6.7	0.76
0.09	96.9	54.8	3.5	7.5	0.67
0.06	99.6	54.2	1.6	9.2	0.65

Reaction conditions: 1.85 mmol of each reagent, 1.0 g of the catalyst dried 2.0 h at 105°C, temperature 25°C, initial concentration of reagents was reduced by increasing of total volume of reaction mixture

A decrease in the X_2/X_1 ratio with dilution of the reagents (Table 6) may indicate that terpenoid **1** undergoes side transformations if the reaction order different from the main reaction. Indeed, when the initial concentrations of **1** were 0.09 and 0.06 mol/L, according to GC-MS data, 3,4-dimethylcumene was formed, apparently as a result of dehydration and aromatization (Fig. S5a). With an increase of the reaction mixture volume, a decrease in the selectivity to isobenzofurans **4** and

an increase in selectivity to products **5** were also observed, which indicates the dehydration of compounds **4** into **5** (Fig. S4b).

Thus, with a decrease in the initial concentration of **1**, the contribution of monomolecular reactions (dehydration) became more pronounced, which led to a decrease in the yield of the bimolecular condensation product **3**. Dependences of the selectivity for xanthene **3** on the conversion of terpenoid **1** and on its initial concentrations are shown in Fig. 7.

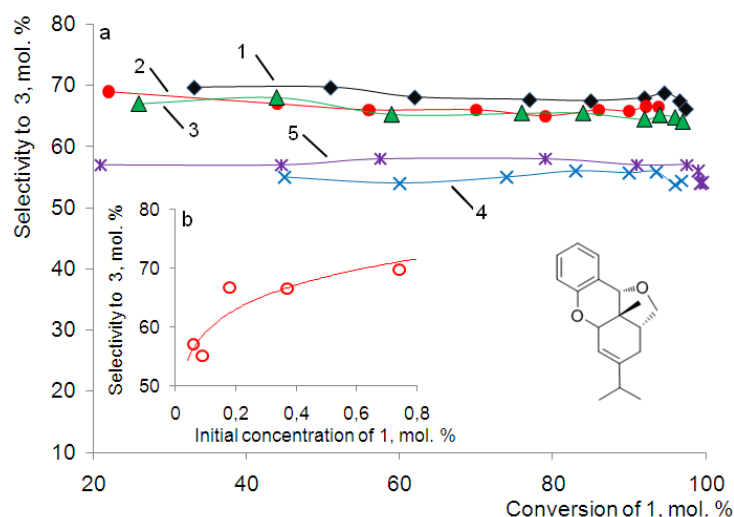


Fig. 7. Selectivity to xanthene **3** as a function of terpenoid **1** conversion (a) and its initial concentration for 5 h (b, see insert), mol/l: 0.74 (1); 0.37 (2); 0.18 (3); 0.09 (4) and 0.06 (5))

A very simplistic kinetic view of the reaction mechanism implies parallel formation of xanthene **3** and compounds **4** and **5** in bimolecular reactions, while dehydration of **1** to 3,4-dimethylcumene is a monomolecular reaction leading to the following expression of differential selectivity S_3

$$\begin{aligned}
 S_3 &= \frac{k_{1 \rightarrow 3} C_1 C_2}{k_{1 \rightarrow 3} C_1 C_2 + k_{1 \rightarrow 4} C_1 C_2 + k_{1 \rightarrow 5} C_1 C_2 + k_{1 \rightarrow \text{cumene}} C_1} = \\
 &= \frac{\frac{k_{1 \rightarrow 3}}{k_{1 \rightarrow \text{cumene}}} C_2}{\frac{k_{1 \rightarrow 3} + k_{1 \rightarrow 4} + k_{1 \rightarrow 5}}{k_{1 \rightarrow \text{cumene}}} C_2 + 1} \quad (1)
 \end{aligned}$$

where C_1 and C_2 are concentrations of components **1** and **2** respectively, while k_i are rate constants. At a very low concentration of the terpenoid **1** and thus the corresponding aldehyde **2** the term in the denominator in eq. (1) containing concentration of the aldehyde is lower than unity implying an increase of selectivity with the concentration increase. A more rigorous numerical analysis based on

the mechanism described in the subsequent section is planned in the future to verify the kinetic hypothesis in a more quantitative fashion.

3.2.2 Mechanistic discussion

According to the proposed mechanism of the *trans*-4-hydroxymethyl-2-carene **1** reaction with salicylic aldehyde **2** (Fig. 8), the protonated form of **2** interacts with **1** at the first stage (Prins reaction), leading to formation of the intermediate **3-A**, subsequent opening of the cyclopropane ring in which gives the cation **3-B**. Cyclization of this ion with the intramolecular water transfer leads to formation of isobenzofuran alcohols **4**. However, the main pathway of the **3-B** transformation involves formation of cation **3-C**, which reacting further with the nucleophile (-OH) by an intramolecular cascade reaction gives the xanthene product **3**. An alternative pathway for the **3-C** transformation is cyclization and deprotonation giving isobenzofuran products **5** as a result (Fig. 8).

A decrease in selectivity to xanthene **3** with a decrease in the initial concentration of terpenoid **1** (Fig. 7) is due to dehydration and aromatization reaction in these conditions (Fig. 8b). In addition, at low initial concentrations of **1**, dehydration of **4** into **5** was also observed (Table 6, Fig. S5).

The yield of xanthene **3** increased with an increase in the clays acidity (Table 3), as well as the drying temperature (Tables 4 and S2). On strong Brønsted and Lewis acid (Amberlyst-15, BF₃·Et₂O) low selectivity to **3** was observed (Table 3). Moreover, over Amberlyst-15 3,4-dimethylcumene was also formed (Fig. 8b). Consequently, the Prins cascade reaction is effectively catalyzed by materials with medium acidity (*ca.* 100 μmol/g), in particular commercial montmorillonites K-10 and K-30 (Table 3).

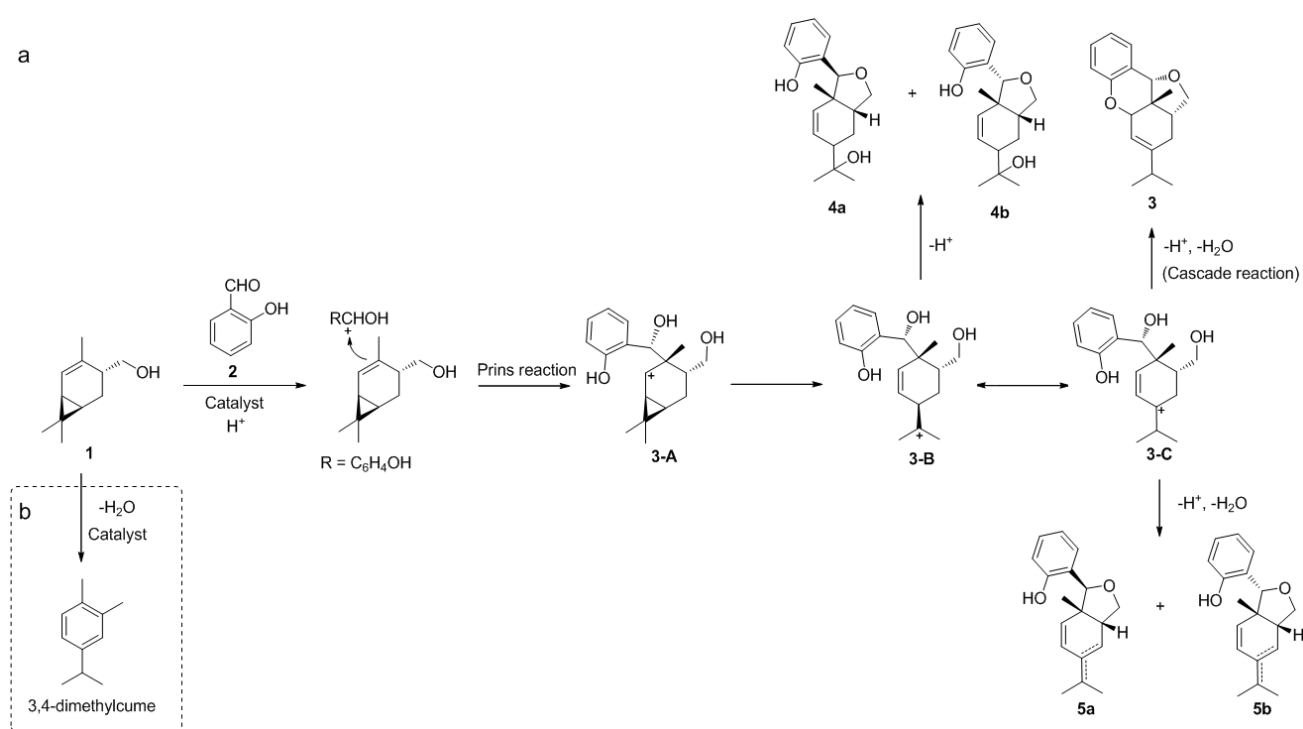


Fig. 8. The mechanism of the cascade Prins reaction of 4-*trans*-hydroxymethyl-2-carene **1** with salicylic aldehyde (a) and a scheme of the compound **1** aromatization (b)

In contrast to the cascade reaction studied in this work, during the Prins condensation of terpenoid (-)-isopulegol with thiophene-2-carbaldehyde (Fig. S7a), selectivity to octahydro-2*H*-chromen-4-ol increased with a decrease in the catalyst acidity and its drying temperature [32]. This was explained by formation of a cyclic intermediate on weak a.s. of halloysite nanotubes with H₂O transfer from their surface to the intermediate, leading to the formation of diastereomeric alcohols [36].

According to [33], the Prins condensation on aluminosilicate catalysts proceeds through transition states with a partial proton transfer, which become full ion pairs only in the presence of the strongest acids. It can be assumed that the key stage of the cascade reaction, namely the intramolecular addition of the hydroxyl group (**3-C** to **3**, Fig. 8), requires a larger positive charge on the cation center than in the case of water transfer (Fig. S7a), which efficiently proceeds at weak acid sites. Similarly, in the (-)-isopulegol reaction with acetone, the formation of an ester was observed as a product of the addition of the second molecule of this terpenoid to the carbocation (Fig. S7b), and the selectivity to ester increased with increasing acidity and the catalyst drying temperature [55]. Also note that the tandem Prins-Ritter reaction proceeded efficiently on stronger Brønsted acids (SO₃H-modified solids, *p*-toluenesulfonic acid) [29].

3.3. Cascade Prins-Friedel-Crafts reaction

3.3.1. Influence of catalyst type and reaction conditions

Condensation of *trans*-4-hydroxymethyl-2-carene **1** with 3,4,5-trimethoxybenzaldehyde **6** in the presence of the studied clays led to formation of a polycyclic compound with a fluorenofuran structure **7** (a product of the Prins-Friedel-Crafts reaction) as well as isobenzofurans **8** as two stereoisomers (Fig. 9). In addition, formation of a number of compounds with unidentified structure was observed (Fig. S2b), having, according to GC-MS, the value $m/z = 344$ (i.e. isomers of product **7**).

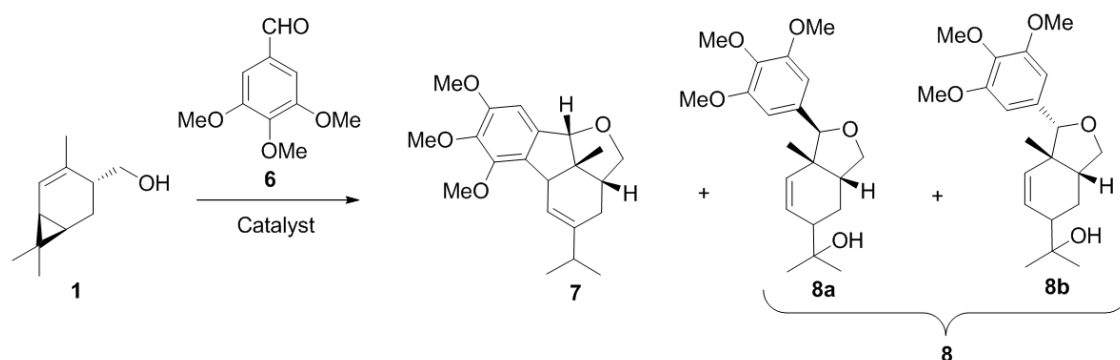


Fig. 9. Products of the *trans*-4-hydroxymethyl-2-carene reaction with 3,4,5-trimethoxybenzaldehyde

At 50% conversion of terpenoid **1**, selectivity towards polycyclic compound **7** in the presence of montmorillonite K-10 (78.3%) was higher than that over illite and halloysite (Table 7). The largest selectivity to isobenzofuran compounds **8** (10.8%) was observed for illite clay, with the compound **8b** predominating in all cases (Table 7). Note that the conversion of terpenoid **1** (X_1) was higher than that for aldehyde **6** (X_6), which indicates that **1** was involved in side transformations.

Table 7. Acidity and catalytic properties of the studied catalysts in *trans*-4-hydroxymethyl-2-carene reaction* with 3,4,5-trimethoxybenzaldehyde

Catalyst	Acidity, $\mu\text{mol/g}$	r_0 , $\text{mmol}/(\text{g}\cdot\text{min})$	TOF, min^{-1}	Time, min	Selectivity, mol. %		8b/8a	X_2/X_1
					7	8		
Halloysite	52	0.22	4.2	30	73.8	7.2	14.1	0.84
Illite	63	0.08	1.2	300	57.2	10.8	2.5	0.57
K-10	104	0.40	3.9	15	78.3	5.9	9.3	0.91
K-30	100	0.33	3.3	15	78.1	6.2	9.3	0.90
$\text{BF}_3\cdot\text{Et}_2\text{O}^{**}$	-	-	-	180	51.4	11.3	4.3	0.90
Amberlyst-15	-	0.30	-	10	6.7	-	-	0.43
H-Beta-300	112.0	No condensation						

Reaction conditions: 1.85 mmol of each reagent, 1.0 g of the catalyst dried 2.0 h at 105°C , temperature 25°C , initial concentration of reagents was 0.37 mol/l. *At ca. 50% conversion, **1.0 eq, at 0°C and 23.4%

Both the initial consumption rate of terpenoid **1** and selectivity to the desired product **7** were the highest on montmorillonites K-10 and K-30, which are characterized by the largest acidity among clays (*ca.* 100 $\mu\text{mol/g}$, Table 7). The highest TOF values were observed for HNT and K-10. On the other hand, in the presence of Amberlyst-15 and Lewis $\text{BF}_3 \cdot \text{Et}_2\text{O}$, the yield of polycyclic compound **7** did not exceed 51.4%. The reaction mixture obtained on Amberlyst-15 also contained 3,4-dimethylcumene, which was formed as a result of dehydration and aromatization reactions of the starting compound **1** (Fig. S5a). Over zeolite H-Beta-300, no reaction was observed (Table 7), which may be due to its small pore size (0.76 nm according to [40]).

Note that after 5 h of the reaction, the highest conversion of terpenoid **1** (90.4%, Table S3) was also observed in the presence of montmorillonite catalysts. At the same time, selectivity to the products **7** and **8** practically did not depend on conversion (Fig. S8).

Proceeding from this, as in the case of the Prins cascade condensation (Fig. 5), the Prins-Friedel-Crafts reaction is more efficiently catalyzed by mesoporous montmorillonite clays with medium total concentrations of Brønsted and Lewis a.s. (*ca.* 100 $\mu\text{mol/g}$). The conclusions obtained in this work are consistent with the results of [31], which reported that mesoporous hierarchical Beta zeolites with acidity in the range between 90 and 200 $\mu\text{mol/g}$ are suitable catalysts for the one-pot synthesis of 4-aryltetrahydropyran compounds from butyraldehyde, 3-butene-1-ol and anisole.

With an increase in the drying temperature of K-10, the initial consumption rate of *trans*-4-hydroxymethyl-2-carene **1** sharply increased, being the highest after heat treatment at 150°C (Table 8). Selectivity to product **7** also increased, reaching 83.6% when the catalyst was dried at 200°C, while the yield of isobenzofuran compounds **8** decreased to 4.3%. Under these conditions, almost complete transformation of reagent **1** was observed (Table 8).

Based on the fact that montmorillonite possesses the highest Brønsted acidity after heat treatment at 150°C, while the highest Lewis acidity occurs at 250 and 300°C [54], the occurrence of Prins-Friedel-Crafts reaction is favored by relatively strong a.s. of both types arising in these conditions of clay drying.

Table 8. Selectivity in *trans*-4-hydroxymethyl-2-carene reaction with 3,4,5-trimethoxybenzaldehyde on K-10 at 25°C after 5 h

K-10 drying temperature, °C	r_0 , mmol/(g·min)	Conversion of 1 , mol. %	Selectivity, mol. %		X_6/X_1
			7	8	
50	0.005	35.3	62.1	10.0	0.75
105	0.40	90.3	78.6	6.3	0.87

150	0.73	97.6	82.9	4.4	0.92
200	0.71	97.8	83.6	4.3	0.92
350	0.61	95.6	81.1	5.2	0.88
Reaction conditions: 1.85 mmol of each reagent, 1.0 g of the catalyst, temperature was 25°C, initial concentration of reagents was 0.37 mol/l					

A decrease in the initial concentration of *trans*-4-hydroxymethyl-2-carene **1** from 0.74 to 0.06 mol/L led to an increase in the selectivity to polycyclic product **7** from 76.9 to 91.3%, respectively (Table 9, Fig. 10). In this case, a decrease in the isobenzofurans **8** yield from 6.6 to 1.2% was also observed. It should be noted that at low concentrations of **1** (0.06 and 0.09 mol/L), almost complete conversion of this terpenoid was observed already after 1 h of the reaction (Fig. 11).

Table 9. Selectivity in *trans*-4-hydroxymethyl-2-carene reaction with 3,4,5-trimethoxybenzaldehyde after 3 h on K-10 with the different reagents initial concentration

Initial concentration of 1 , mol/L	Conversion of 1 , mol. %	Selectivity, mol. %		X_6/X_1
		7	8	
0.74	89.9	76.9	6.6	0.84
0.37	85.2	78.2	6.3	0.88
0.18	93.1	83.5	4.6	0.89
0.09	98.7	88.1	2.7	0.91
0.06	99.3	91.3	1.2	0.93
Reaction conditions: 1.85 mmol of each reagent, 1.0 g of the catalyst dried 2.0 h at 105°C, temperature 25°C, initial concentration of reagents was reduced by increasing of total volume of reaction mixture				

An increase in selectivity to product **7** with a decrease in the initial concentration of **1** (Table 12, Fig. 10) may be because of monomolecular transformations of isobenzofurans **8**, as well as other formed products (Fig. S2) into this polycyclic compound, as indicated by a decrease in the yield of **8** with increasing the reaction mixture volume (Table 9). Indeed, in the presence of clay K-10, isobenzofurans **8**, as well as a mixture of unidentified products with $m/z = 344$, which were isolated by column chromatography, were converted to compound **7** (Fig. S9). Based on this, an increase in the yield of **7** upon dilution occurs by isomerization/dehydration of by-products to this substance.

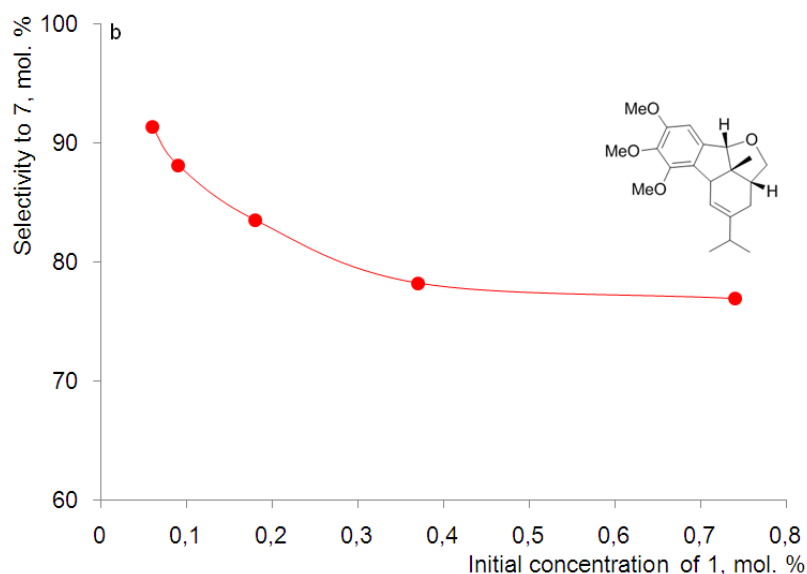


Fig. 10. Selectivity to product 7 as function of terpenoid 1 initial concentration

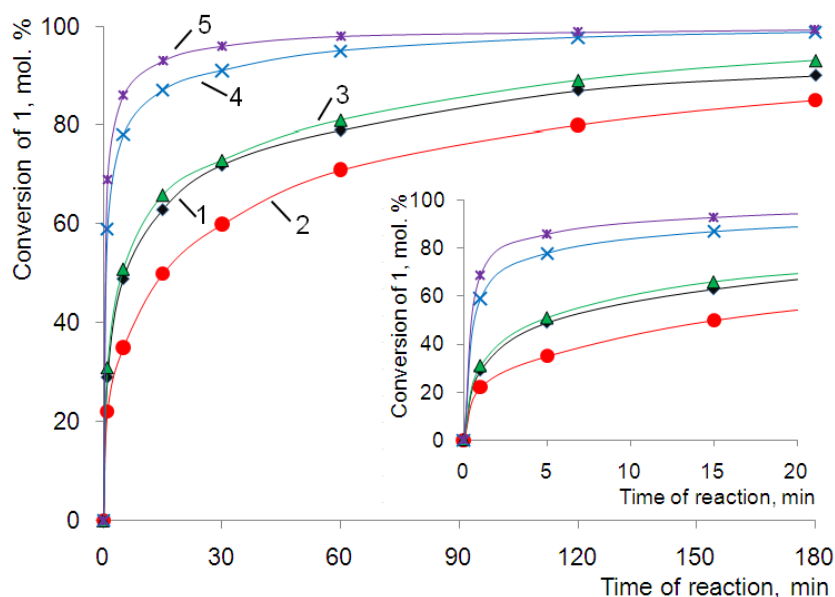


Fig. 11. Conversion of terpenoid 1 as function of reaction time at its initial concentration, mol/l: 0.74 (1); 0.37 (2); 0.18 (3); 0.09 (4) and 0.06 (5)

It is important to note that the dependences of selectivity to polycyclic products of the Prins (Fig. 7b) and Prins-Friedel-Crafts cascade reaction (Fig. 10) on the *trans*-4-hydroxymethyl-2-carene 1 initial concentration had an opposite character. Thus, during condensation of 1 with salicylic aldehyde 2 in dilute solutions (0.06 and 0.09 mol/L), a side reaction of the starting compound dehydration/aromatization to 3,4-dimethylcumene occurred (Fig. 8b), which was not observed in the case of its condensation with 3,4,5-trimethoxybenzaldehyde 6. This can be explained by much faster reaction of 1 with aldehyde 6 than with reagent 2, which is clearly seen from the kinetic curves (Fig. S6 and 11).

3.3.2 Mechanistic discussion and DFT study

The proposed mechanism for terpenoid **1** reaction with 3,4,5-trimethoxybenzaldehyde **6** is shown in Fig. 12. Initially, the protonated form of aldehyde reacts with the electrophilic carbon atom in **1** (the Prins reaction) leading to formation of the intermediate **7-A**, which, through the opening of the cyclopropane ring gives the carbocation **7-B**. Subsequently, this intermediate is transformed into **7-C**, which interacts intramolecularly with an aromatic ring (the Friedel-Crafts reaction) to give the desired polycyclic compound **7** (Fig. 12). In an alternative direction, **7-B** undergoes cyclization with the transfer of water to the isopropyl fragment, which leads to the formation of the isobenzofuran compounds **8**.

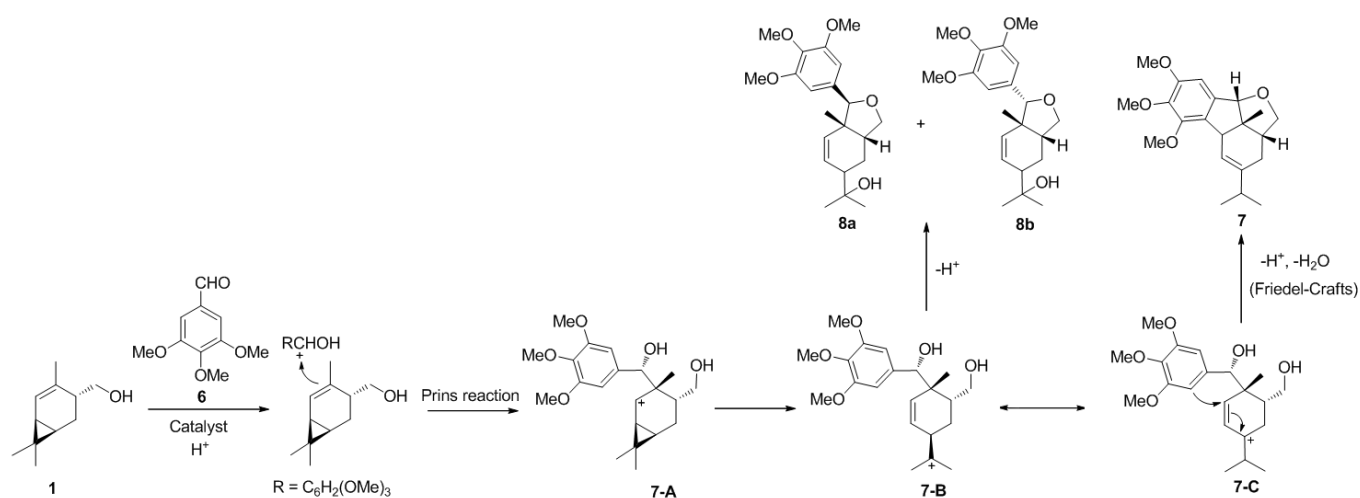


Fig. 12. The mechanism of the cascade Prins-Friedel-Crafts reaction of *trans*-4-hydroxymethyl-2-carene with 3,4,5-trimethoxybenzaldehyde

A more detailed evaluation of the reaction mechanism was performed using DFT calculations. Thus, the secondary carbocation **7-A** is formed from the reagents with a relatively higher energy 59.2 kJ/mol, Fig. 13). With its further transformation through opening of the cyclopropane ring formation of the tertiary carbocation **7-B** occurs, which is stabilized because of hyperconjugation effects. Particularly, a difference of *ca.* 64 kJ/mol with the carbocation **7-A** led to significant differences in terms of reactivity and stability. Similar trend was also observed when the $GAP_{\text{HOMO-LUMO}}$ was calculated at MP2 level of theory (Table S4). In the case of carbocation **1'-A**, a $GAP_{\text{HOMO-LUMO}}$ of 9.51 eV was obtained while for **8-A** was of 9.21 eV. It is well known that $GAP_{\text{HOMO-LUMO}}$ is intimately related with the reactivity of an organic species meaning that a smaller value corresponds to a faster reaction [56]. Thus, the intermediate **7-A** should readily convert to the more stable cation **7-B**.

Following the pathway of **7-B**, further cyclization and OH-transfer is carried out to give the isobenzofurans **8a** and **8b** with a difference of 43.5 kJ/mol (Fig. 13). Conversion of carbocation **7-B** into **8a** and **8b** is favored because of the axial and equatorial positions of the OH groups (Fig. S10). This leads to an increased cyclization rate that limits another reaction (e.g.: C=C formation in the *exo*-tertiary carbocation) as stated previously [57]. Experimentally **8b** was obtained in excess compared to **8a** (Table 7), reflecting better reactivity the equatorial position compared to the axial approach to the possible transition state.

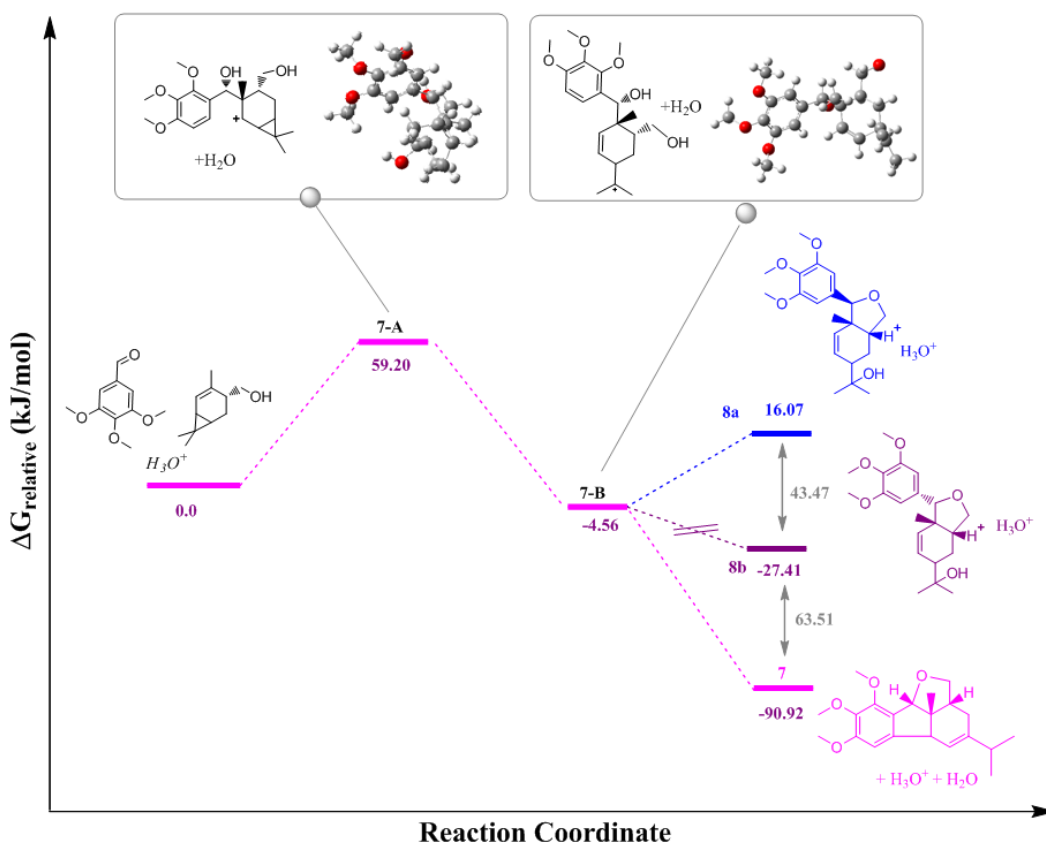


Fig. 13. The DFT profile for terpenoid **1** reaction with 3,4,5-trimethoxybenzaldehyde

According to the main reaction direction (the intramolecular Friedel-Crafts reaction), carbocation **7-C** is formed from **7-B** with a subsequent transformation into the polycyclic product **7** (Fig. 12). The energy for **7** is 86.4 kJ/mol lower than for **7-B** (Fig. 13). Then, with a difference of almost 63.5 and 107 kJ/mol, respectively, polycyclic compound **7** is thermodynamically favored over both **8b** and **8a** isobenzofurans. These data are in complete agreement with the experimentally observed isomerization of compounds **8** to polycyclic product **7** (Fig. S9). Note that the calculated thermodynamic parameters for products **7** and **8a, b** are in complete agreement with the values of the initial rates of formation of these compounds (Table S5).

The sizes of the intermediates and the reaction products are between 1.07 and 1.35 nm (Table S6), which is significantly lower than the pore diameter in the studied clays (5.1–10.1 nm, Table 1). At the same time, zeolite H-Beta-300 did not exhibit catalytic activity in the reaction of **1** with the aldehyde **6**, apparently due to the small pore size (0.76 [40]). Therefore, mesoporosity of the catalyst is one of the key factors determining its efficiency in the Prins-Friedel-Crafts reaction.

Considering that selectivity to heterocycles **7** and **8** does not practically depend on the terpenoid **1** conversion (Fig. S8), these compounds are formed in a parallel fashion. However, with a decrease in the initial concentrations of **1**, an increase in selectivity to the polycyclic compound **7** was observed (Fig. 10) due to isomerization of by-products to this compound (Fig. S9).

Reflecting an increase of the initial consumption rate of **1** and selectivity for polycyclic product **7** with an increase in the catalyst acidity (Table 7), as well as the drying temperature (Table 8), mesoporous montmorillonites with a total acidity of *ca.* 100 $\mu\text{mol/g}$ after thermal treatment at 150–200°C effectively catalyzed the cascade Prins-Friedel-Crafts reaction, affording selectivity towards the desired product **7** up to 91.3% (Table 9). Similarly, hierarchical Beta zeolites with acid site concentrations ranging from 90 to 200 $\mu\text{mol/g}$ are selective catalysts for synthesis of 4-aryltetrahydropyran compounds [31]. On the other hand, in the presence of the strong acid Amberlyst-15, the reagent **1** was dehydrated with the formation of 3,4-dimethylcumene (Fig. S5a).

It is also important to note that when studying the classical Friedel-Crafts reaction of benzene alkylation with benzyl chloride, it was shown that conversion of the latter and selectivity to diphenylmethane increased with increasing acidity of metakaolin used as a catalytic system [58]. In the present work, it was found for the first time that the yield of the product of the Prins-Friedel-Crafts reaction significantly increases with an increase in the acidity and drying temperature of aluminosilicate catalysts, as well as with a decrease in the initial concentration of reagents.

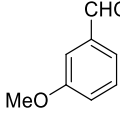
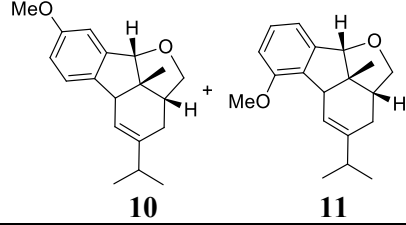
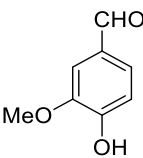
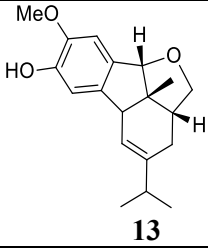
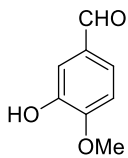
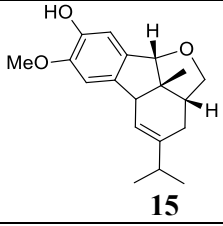
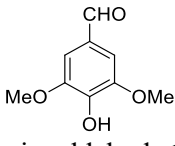
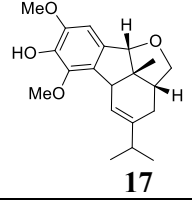
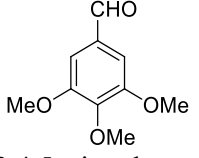
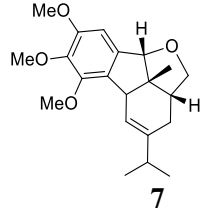
3.3.3 Reaction scope and catalyst reusability

The terpenoid **1** reaction with a number of substituted aldehydes was studied on clay K-10 dried at 200°C and the initial concentration of reagents equal to 0.06 mol/L.

It is known [13] that the condensation of **1** with benzaldehyde leads to formation of a complex mixture of products, from which isobenzofurans were isolated (34%, Fig. S11). According to the results of this work, when 3-methoxybenzaldehyde **9** was used, polycyclic products of the Prins-Friedel-Crafts reaction **10** and **11** were formed with a total selectivity of 92.7% and **10/11** isomer ratio of 5.0 (Table 10, entry 1). Note that similar products, differing in the position of the methoxy group, were observed upon condensation of aldehyde **9** with *trans*-4-phenyl-but-3-en-1-ol [15]. Thus, the presence of an electron-donor substituent in the meta-position of benzaldehyde is a key factor for the occurrence of this type of cascade reactions.

An increase in the number of substituents (hydroxy and methoxy groups) in the 3,4 and 5 positions of benzaldehyde leads to formation of only one condensation product and an increase in its yield, which in the case of syringaldehyde **16** reaches 97.0% (Table 10, entry 4). It should be noted that selectivity of the compound **1** reaction with isovanillin to product **15** (80.9%, table 10, entry 3), which has a high cytotoxic activity, is significantly higher than the yield (49.0%) obtained previously [13].

Table 10. Selectivity in *trans*-4-hydroxymethyl-2-carene* reaction with a number of aldehydes on montmorillonite K-10

Entry	Aldehyde	Time, min	Products	Selectivity, mol. %
1	 3-methoxybenzaldehyde 9	60	 10 + 11	92.7 (5:1)
2	 Vanillin 12	60	 13	87.7
3	 Isovanillin 14	60	 15	80.9
4	 Syringaldehyde 16	120	 17	97.0
5	 3,4,5-trimethoxybenzaldehyde 6	60	 7	94.0

Reaction conditions: 1.85 mmol of each reagent, 1.0 g of catalyst dried 2.0 h at 200°C, temperature was 25°C, initial concentration of reagents was 0.06 mol/l. *At 99% conversion

Thus, carrying out the cascade Prins-Friedel-Crafts reaction in the presence of montmorillonite K-10 heat-treated at 200°C and low concentrations of reagents makes it possible to obtain the desired polycyclic products with very high selectivity (up to 97.0%).

Although clays are cheap and non-toxic materials, a possibility of reusing montmorillonite K-10 in *trans*-4-hydroxymethyl-2-carene **1** condensation with 3,4,5-trimethoxybenzaldehyde **6** has been evaluated. For this purpose, the catalyst was separated from the reaction mixture, washed with ethyl acetate (3 times x 7 mL x 10 min), distilled water and dried for 2 h at 105°C. Immediately before the reaction, K-10 also was treated at 200°C for 2 h. The catalyst activity and selectivity for the polycyclic product **7** in the second cycle of its use remained practically unchanged (Table 11). The kinetic curves for the compound **1** conversion in the first and second reaction cycles are shown in Fig. S12. After using the K-10 in the reaction cycle, its porous structure did not change (Table 12, Fig. S13). At the same time, a slight decrease in the concentration of acid sites was observed.

Table 11. Selectivity in *trans*-4-hydroxymethyl-2-carene reaction with 3,4,5-trimethoxybenzaldehyde on montmorillonite K-10 for 1 h

Cycle of utilization K-10	Conversion of terpenoid 1 , mol. %	Selectivity, mol%		X_6/X_1
		7	8	
1 (fresh)	99.0	94.0	1.0	0.95
2	96.0	93.0	1.1	0.95

Reaction conditions: 1.85 mmol of each reagent, 1.0 g of catalyst dried 2.0 h at 200°C, temperature 25°C, initial concentration of reagents was 0.06 mol/l. *At 99% conversion

Table 12. Physico-chemical properties of montmorillonite K-10 after use in the reaction

K-10	Porous structure			Acidity, $\mu\text{mol/g}$
	S_{BET} , m^2/g	V_{pore} , cm^3/g	D_{pore} , nm	
Fresh	247	0.36	5.1	104.0
After reaction cycle	245	0.33	5.6	95.0

An additional study the catalyst stability showed that after 4 reaction cycles there was a slight decrease in the conversion of compound **1** and selectivity to **7**, but these values were still at a high level (Fig. 14). Thus, commercial montmorillonite exhibits good stability in the Prins-Friedel-Crafts cascade reaction.

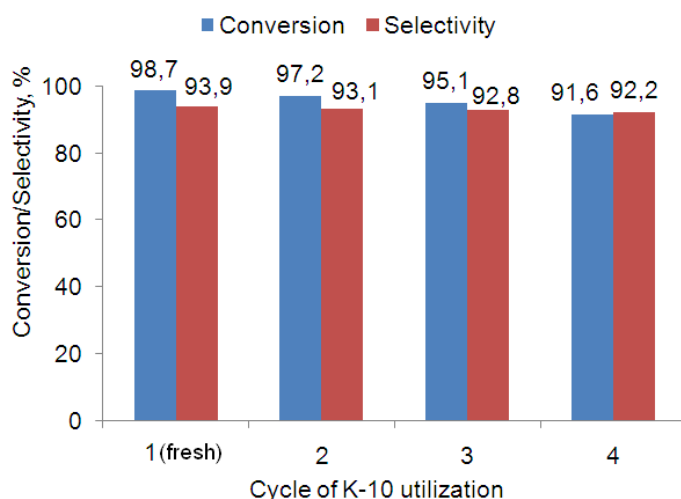


Fig. 14. Conversion of substrate 1 and selectivity to product 7 depending on reaction cycles

Conclusions

The Prins and the Prins-Friedel-Crafts cascade reactions were studied for the first time in terpenoid *trans*-4-hydroxymethyl-2-carene condensation with aromatic aldehydes on mesoporous acidic halloysite, illite, and montmorillonite clays. The investigated terpenoid was synthesized from (+)-3-carene, one of the main components of gum turpentine. The catalysts were well characterized by EDX, SEM, FTIR with pyridine, N₂ adsorption-desorption methods.

Over the studied clays, the main products of the terpenoid reaction with salicylic aldehyde (the Prins cascade) were the xanthene derivative, while in the case of 3,4,5-trimethoxybenzaldehyde (the Prins-Friedel-Crafts reaction), the polycyclic compound with a tetrahydrofuran moiety was formed. Compounds with a benzofuran core were also observed in smaller amounts.

In both reaction types, the initial rate of the starting reagent consumption and selectivity to the desired polycyclic products increased with an increase in the clays acidity. Commercial montmorillonites K-10 and K-30, which are characterized by a moderate concentration of acid sites (*ca.* 100 μmol/g), showed the highest selectivity to polycyclic compound (78%). The target products yield also increased with an increase in the K-10 drying temperature, reaching 84% after treatment at 200°C, which indicates that the relatively strong Brønsted and Lewis acid sites of clays effectively catalyze the reactions. On the other hand, on traditional catalysts (BF₃·Et₂O, Amberlyst-15) the polycycles yields did not exceed 51% due to side reactions. Acidic zeolite Beta-300 did not show any activity due to the small pore size (0.76 nm) compared to that for molecules (1.07–1.35 nm), which means that the mesoporosity of the catalyst is a key factor for the studied reactions.

In the Prins reaction of *trans*-4-hydroxymethyl-2-carene with salicylic aldehyde, the yield of the xanthene decreased with a decrease in the initial terpenoid concentration by its partial conversion

to 3,4-dimethylcumene under these conditions. On the contrary, when the 3,4,5-trimethoxybenzaldehyde was involved (the Prins-Friedel-Crafts cascade), dilution led to a significant increase in selectivity to the polycyclic product (up to 91%) and its decrease in isobenzofurans due to conversion into the target product.

The mechanisms of the studied reactions were discussed. It was shown by DFT calculations that the reaction of the terpenoid along the Friedel-Crafts pathway is energetically much more favorable than the alternative formation of isobenzofurans. The calculated thermodynamic parameters for products are in complete agreement with the values of the initial rates of formation of these compounds

It was found that the presence of at least an electron-donor substituent at the *m*-position of benzaldehyde is also a key factor in Prins-Friedel-Crafts reaction. The *trans*-4-hydroxymethyl-2-carene reaction with a number of substituted aromatic aldehydes in dilute solutions on K-10 dried at 200°C proceeded with selectivity to the polycyclic products up to 97%. The reusability of K-10 has also been shown. Overall, mesoporous montmorillonites with moderate Brønsted and Lewis acidity can effectively replace homogeneous catalysts for the cascade Prins/Friedel-Crafts reactions.

Acknowledgments

The research was financially supported by Belarusian Republican Foundation for Fundamental Research (BRFFR, grant X20R-001) and Russian Foundation for Basic Research (RFBR, grant 20-53-00004 Bel_a). The authors are grateful to Dr. T.F. Kuznetsova (IGICH of NAS of Belarus) for performing N₂ physisorption and to K. Dubatouka (IChNM of NAS of Belarus) for recording of EDX spectra. J.E. Sánchez-Velandia thanks to Pontificia Universidad Javeriana for providing computational powder.

Conflict of interest

The authors declare that there is no conflict of interest

References

References

1. A. Lorente, J. Lamariano-Merketegi, F. Albericio, M. Álvarez. Tetrahydrofuran-Containing Macrolides: A Fascinating Gift from the Deep Sea. *Chem. Rev.*, 2013, 113, 4567–4610.
3. Q. Lu, D.S. Harmalkar, Y. Choi, K. Lee, An Overview of Saturated Cyclic Ethers: Biological Profiles and Synthetic Strategies. *Molecules*, 24, 2019, 3778.
3. I.V. Il'ina, N.S. Dyrkheeva, A.L. Zakharenko, A.Yu. Sidorenko, N.S. Li-Zhulanov, D.V. Korchagina, R. Chand, D.M. Ayine-Tora, A.A. Chepanova, O.D. Zakharova, E.S. Ilina, J. Reynisson, A.A. Malakhova, S.P. Medvedev, S.M. Zakian, K.P. Volcho, N.F. Salakhutdinov, O.I. Lavrik, Design, synthesis, and biological investigation of novel classes of 3-carene-derived potent inhibitors of TDP1. *Molecules*, 2020, 25, 3496.
4. B. Wang, A.P. Ramirez, J.J. Slade, J.P. Morken, Enantioselective Synthesis of (–)-Sclerophytin A by a Stereoconvergent Epoxide Hydrolysis, *J. Am. Chem. Soc.*, 2010, 132, 16380–16382
5. X. Wang, W. Sun, J. Cao, H. Qu, X. Bi, Y. Zhao, Structures of New Triterpenoids and Cytotoxicity Activities of the Isolated Major Compounds from the Fruit of *Momordica charantia* L. *J. Agric. Food Chem.*, 2012, 60, 3927.
6. H. Abas, S.M. Linsdall, M. Mamboury, H.S. Rzepa, A.C. Spivey, Total Synthesis of (+)-Lophirone H and Its Pentamethyl Ether Utilizing an Oxonium–Prins Cyclization, *Org. Lett.*, 2017, 19, 2486–2489.
7. A.C. Spivey, L. Laraia, A.R. Bayly, H.S. Rzepa, A.J. P. White, Stereoselective synthesis of *cis*- and *trans*-2,3-disubstituted tetrahydrofurans via oxonium-Prins cyclization: access to the Cordigol ring system, *Org. Lett.*, 2010, 12, 900–903.
8. S. Roy, Prins-Friedel-Crafts cyclization: Synthesis of diversely functionalized six-membered oxacycles, *Curr. Org. Chem.*, 2021, 25, 635–651.
9. P. Padmaja, P. Narayana Reddy, B.V. Subba Reddy, Tandem Prins cyclizations for the construction of oxygen containing heterocycles, *Org. Biomol. Chem.*, 2020, 18, 7514–7532.
10. L. Lv, S. Lu, Y. Chen, Z. Li, Diastereoselective building up polycyclic tetrahydrofurans via tandem annulation of 1,n-enynes with aliphatic acids, *Org. Chem. Front.*, 2017, 4, 2147–2152
11. O.S. Patrusheva, K.P. Volcho, N.F. Salakhutdinov, Synthesis of oxygen-containing heterocyclic compounds based on monoterpenoids, *Russ. Chem. Rev.*, 2018, 87, 771–796.
12. N.F. Salakhutdinov, K.P. Volcho, I.V. Il'ina, D.V. Korchagina, L.E. Tatarova, V.A. Barkhash, New reactions of isoprenoid olefins with aldehydes promoted by Al₂O₃-SiO₂ catalysts, *Tetrahedron*, 1998, 54, 15619–15642.
13. S.Yu. Kurbakova, I.V. Il'ina, O.S. Mikhailchenko, M.A. Pokrovsky, D.V. Korchagina, K.P. Volcho, A.G. Pokrovsky, N.F. Salakhutdinov, The short way to chiral compounds with

hexahydrofluoreno[9,1-bc]furan framework: Synthesis and cytotoxic activity. *Bioorg. Med. Chem.*, 23, 2015, 1472–1480.

14. Y. Suzuki, T. Niwa, E. Yasui, M. Mizukami, M. Miyashita, S. Nagumo, Tandem five membered-ring selective Prins reaction and Friedel–Crafts reaction, *Tetrahedron Lett*, 2012, 53, 1337–1340.

15. Y. Sakata, E. Yasui, K. Takatori, Y. Suzuki, M. Mizukami, S. Nagumo, Syntheses of polycyclic tetrahydrofurans by cascade reactions consisting of five-membered ring selective Prins cyclization and Friedel–Crafts Cyclization, *J. Org. Chem.* 2018, 83, 9103– 9118.

16. A. Behr, A.J. Vorholt, K.A. Ostrowski, T. Seidensticker, Towards resource efficient chemistry: tandem reactions with renewable, *Green Chem.*, 2014, 16, 982–1006.

17. J.D. Tibbetts, S.D. Bull, Dimethyl sulfide facilitates acid catalysed ring opening of the bicyclic monoterpenes in crude sulfate turpentine to afford *p*-menthadienes in good yield, *Green Chemistry*, 2021, 23, 597–610.

18. G. Ohloff, H. Farnow, W. Philipp, Homologous alcohols of the terpene and sesquiterpene series. X. Synthesis of (+)-3-hydroxymethyl-4-carene, *Justus Liebigs Ann. Chem.*, 1958, 613, 43–55.

19. M. Zielińska-Błajet, J. Feder-Kubis, Monoterpenes and their derivatives – recent development in biological and medical applications, *Int. J. Mol. Sci.*, 2020, 21, 7078.

20. A.Yu. Sidorenko, I.V. Il'ina, A.V. Kravtsova, A. Aho, O.V. Ardashov, N.S. Li-Zhulanov, K.P. Volcho, N.F. Salakhutdinov, D.Yu. Murzin, V.E. Agabekov, Preparation of chiral isobenzofurans from 3-carene in the presence of modified clays, *Mol. Catal.*, 2018, 459, 38 – 45.

21. Y. Sakata, E. Yasui, M. Mizukami, S. Nagumo, Cascade reaction including a formal [5+2] cycloaddition by use of alkyne-Co₂(CO)₆ complex, *Tetrahedron Lett.*, 2019, 60, 755–759.

22. R.J. Hinkle, S.E. Lewis, Atom economical, one-pot, three-reaction cascade to novel tricyclic 2,4-Dihydro-1*H*-benzo[*f*]isochromenes, *Org. Lett*, 2013, 15, 4070–4073.

23. P. Rajasekaran, Y. Mallikharjunarao, Y.D. Vankar, Synthesis of 1*C*-Aryl/Alkyl 2*C*-Branched Sugar-Fused Isochroman Derivatives by Sequential Prins and Friedel–Crafts Cyclizations on a Perlin Aldehyde Derived Substrate, *Synlett*, 2017, 28, 1346–1352.

24. J. S. Yadav, B.V. Subba Reddy, K. Ramesh, G.G.K.S. Narayana Kumar, R. Grée, A novel aza-Prins-Friedel-Crafts reaction for the synthesis of 4-arylpiperidines, *Tetrahedron Lett.*, 2010, 51, 818–821.

25. E. Fenster, C. Fehl, J. Aubé, Use of a tandem Prins/Friedel-Crafts reaction in the construction of the indeno-tetrahydropyridine core of the haouamine alkaloids: formal synthesis of (-)-Haouamine A, *Org. Lett*, 2011, 13, 2614–2617.

26. A. Venkateswarlu, M. Kanakaraju, A.C. Kunwar, Y.V. Rami Reddy, B.V.S. Reddy, Domino Prins cyclization of enynols: stereoselective synthesis of bicyclic vinyl fluorides, *Eur. J. Org. Chem.*, 2015, 5389–5392.

27. C.D.-T. Nielsen, W.J. Mooij, D. Sale, H.S. Rzepa, J. Burés, A.C. Spivey, Reversibility and reactivity in an acid catalyzed cyclocondensation to give furanochromanes – a reaction at the ‘oxonium-Prins’ vs. *ortho*-quinone methide cycloaddition’ mechanistic nexus, *Chem. Sci.*, 2019, 10, 406–412.
28. B. V. Subba Reddy, P. Borkar, J.S. Yadav, B. Sridha, R. Grée, Tandem Prins/Friedel–Crafts cyclization for stereoselective synthesis of heterotricyclic systems, *J. Org. Chem.*, 2011, 76, 7677–7690.
29. A.Yu. Sidorenko, N.S. Li-Zhulanov, P. Mäki-Arvela, T. Sandberg, A.V. Kravtsova, A.F. Peixoto, C. Freire, K.P. Volcho, N.F. Salakhutdinov, V.E. Agabekov, D.Yu. Murzin, Stereoselectivity inversion by water addition in the tandem Prins-Ritter reaction for synthesis of 4-amidotetrahydropyran derivatives, *ChemCatChem*, 2020, 12, 2605–2609.
30. M. R. Dintzner, Montmorillonite K10 clay catalyzed synthesis of 4-aryltetrahydropyrans: a one-pot, multicomponent, environmentally friendly Prins–Friedel–Crafts-type reaction, *Synlett*, 2013, 24, 1091–1092.
31. R. Barakov, N. Shcherban, P. Yaremov, I. Bezverkhy, J. Čejka, M. Opanasenko, Hierarchical Beta zeolites as catalysts in a one-pot three-component cascade Prins–Friedel–Crafts reaction, *Green Chem.*, 2020, 22, 6992–7002.
32. A.Yu. Sidorenko, A.V. Kravtsova, A. Aho, I. Heinmaa, H. Pazniak, K.P. Volcho, N.F. Salakhutdinov, D.Yu. Murzin, V.E. Agabekov, Highly selective Prins reaction over acid-modified halloysite nanotubes for synthesis of isopulegol-derived 2*H*-chromene compounds, *J. Catal.*, 2019, 374, 360 – 377.
33. S. Wang, E. Iglesia, Mechanism of Isobutanal – Isobutene Prins Condensation Reactions on Solid Brønsted Acids, *ACS Catal.* 2016, 6, 7664 – 7684.
34. G. Nagendrappa, Organic synthesis using clay and clay-supported catalysts, *Appl. Clay Sci.*, 2011, 53, 106–138.
35. B.S. Kumar, A. Dhakshinamoorthy, K. Pitchumani, K10 montmorillonite clays as environmentally benign catalysts for organic reactions, *Catal. Sci. Technol.*, 2014, 4, 2378–2396.
36. P. Komadel, Acid activated clays: Materials in continuous demand, *Appl. Clay Sci.*, 2016, 131, 84–99.
37. M. Massaro, R. Noto, S. Riela, Past, Present and future perspectives on halloysite clay minerals, *Molecules*, 2020, 25, 4863.
38. A.Yu. Sidorenko, A.V. Kravtsova, P. Mäki-Arvela, A. Aho, T. Sandberg, I.V. Il'ina, N.S. Li-Zhulanov, D.V. Korchagina, K.P. Volcho, N.F. Salakhutdinov, D.Yu. Murzin, V.E. Agabekov. Synthesis of isobenzofuran derivatives from renewable 2-carene over halloysite nanotubes, *Mol. Catal.*, 2020, 490, 110974.

39. E.P. Barrett, L.G. Joyner, P.P. Halenda, The Determination of Pore Volume and Area Distributions in Porous Substances. *J. Am. Chem. Soc.*, 1951, 73, 373–380.
40. A. Aho, N. Kumar, K. Eränen, T. Salmi, M. Hupa, D.Yu. Murzin, Catalytic pyrolysis of woody biomass in a fluidized bed reactor: Influence of the zeolite structure, *Fuel*, 2008, 87, 2493–2501.
41. A.Yu. Sidorenko, A.V. Kravtsova, A. Aho, I. Heinmaa, T.F. Kuznetsova, D.Yu. Murzin, V.E. Agabekov, Catalytic isomerization of α -pinene oxide in the presence of acid-modified clays, *Mol. Catal.* 2018, 448, 18–29.
42. C.A. Emeis, Determination of Integrated Molar Extinction Coefficients for Infrared absorption bands of pyridine adsorbed on solid acid catalysts, *J. Catal.*, 1993, 141, 347–354.
43. M. Ernzerhof, G.E. Scuseria, Assessment of the Perdew-Burke-Ernzerhof exchange-correlation functional, *J. Chem. Phys.*, 1999, 110, 5029–5036.
44. K.E. Riley, B.T. Op't Holt, K.M. Merz, Critical Assessment of the Performance of Density Functional Methods for Several Atomic and Molecular Properties, *J. Chem. Theory Comput.*, 2007, 3, 407–433.
45. L.A. Curtiss, K. Raghavachari, P.C. Redfern, J.A. Pople, Assessment of Gaussian-2 and density functional theories for the computation of enthalpies of formation, *J. Chem. Phys.*, 1997, 106, 1063–1079.
46. W. Reckien, F. Janetzko, M.F. Peintinger, T. Bredow, Implementation of empirical dispersion corrections to density functional theory for periodic systems, *J. Comput. Chem.*, 2012, 33, 2023–2031.
47. S. Grimme, J. Antony, S. Ehrlich, H. Krieg, A consistent and accurate ab initio parametrization of density functional dispersion correction (DFT-D) for the 94 elements H-Pu, *J. Chem. Phys.*, 2010, 132, 154104.
48. N. Mardirossian, M. Head-Gordon, How Accurate Are the Minnesota Density Functionals for Noncovalent Interactions, Isomerization Energies, Thermochemistry, and Barrier Heights Involving Molecules Composed of Main-Group Elements?, *J. Chem. Theory Comput.*, 2016, 12, 4303–4325.
49. M.E.S. Lind, F. Himo, Theoretical study of reaction mechanism and stereoselectivity of arylmalonate decarboxylase, *ACS Catal.*, 2014, 4, 4153–4160.
50. F. Bergaya, G. Lagaly, Handbook of clay science, Part A: Fundamental, 2013, Elsevier, Amsterdam.
51. I. Tkáč, P. Komadel, D. Müller, Acid-treated montmorillonites – a study by ^{29}Si and ^{27}Al MAS NMR, *Clay Min.*, 1994, 29, 11–19.
52. M. Stekrova, P. Mäki-Arvela, N. Kumar, E. Behraves, A. Aho, Q. Balme, K.P. Volcho, N.F. Salakhutdinov, D.Yu. Murzin, Prins cyclization: Synthesis of compounds with tetrahydropyran moiety over heterogeneous catalysts, *J. Mol. Catal. A: Chem.*, 2015, 410, 260–270.

53. S. Yariv, H. Cross, *Organo-Clay Complexes and Interactions*. Marcel Dekker, New York, 2002.
54. D.R. Brown, C.N. Rhodes, Brønsted and Lewis acid catalysis with ion-exchanged clays, *Catal. Lett.*, 1997, 45, 35–40.
55. A.Yu. Sidorenko, A.V. Kravtsova, I.V. Il'ina, J. Wärnå, D.V. Korchagina, Yu.V. Gatilov, K.P. Volcho, N.F. Salakhutdinov, D.Yu. Murzin, V.E. Agabekov, Clay nanotubes catalyzed solvent-free synthesis of octahydro-2*H*-chromenols with pharmaceutical potential from (-)-isopulegol and ketones. *J. Catal.*, 2019, 380, 145 – 152.
56. R.G. Pearson, Recent advances in the concept of hard and soft acids and bases, *J. Chem. Educ.*, 1987, 64, 561–567.
57. X. Han, G. Peh, P.E. Floreancig, Prins-type cyclization reactions in natural product synthesis, *European J. Org. Chem.*, 2013, 1193–1208.
58. K.R. Sabu, R. Sukumar, R. Rekha, M. Lalithambika, M. (1999). A comparative study on H₂SO₄, HNO₃ and HClO₄ treated metakaolinite of a natural kaolinite as Friedel–Crafts alkylation catalyst. *Catal. Today*, 1999, 49, 321– 326.